New concepts of symmetry for copulas

Benedikt Mangold
University of Erlangen-Nürnberg

New concepts of symmetry for copulas

Benedikt Mangold[1]

University of Erlangen-Nürnberg, Department of Statistics and Econometrics, Lange Gasse 20, 90403 Nürnberg, Germany

Wednesday 10th May, 2017

Abstract

This paper introduces two new concepts of symmetry for multivariate copulas with a focus on tails regions. Properties of the symmetry concepts are investigated for bivariate copulas and a connection to radial symmetry is established. Two nonparametric testing procedures for the new concepts are developed using a vector of locally most powerful rank test statistics, applied to a new generalization of the FGM copula which parameterizes every vertex of the unit cube. This vector quantifies deviations from independence in each vertex and the tests for the new symmetry concepts are based on comparisons of these deviations. It is shown that one of the new tests can also be used to test for radial symmetry, which results in a similar power of detecting bivariate radial symmetry compared to recently published nonparametric tests. Further, an application to insurance data is provided. Finally, an improvement of the selection process in the context of vine copula fitting is proposed that is based on the elimination of copula families with unsuitable symmetry properties.

Keywords: Radial symmetry, vertex symmetry, diametrical symmetry, copula, vine copula, rank-based inference

---

1. Introduction

The rise of copulas, especially vine copulas, has had a huge impact on statistical modeling. Copulas allow flexible modeling of complex dependency structures by connecting many arbitrary univariate marginal distributions to high dimensional probability distribution models. Fields of research in which copulas are frequently applied are for example hydrology (Genest et al., 2007; Gyasi-Agyei, 2011), financial application (e.g. Brechmann et al. (2012); Brechmann and Czado (2013); Low et al. (2013); Weiß and Supper (2013); Lau et al. (2016); Stübinger et al. (2016)), and actuarial risk-modeling (Frees and Valdez, 1998; Guégan and Maugis, 2010; Guégan and Hassani, 2013).

This paper focuses on copulas with absolutely continuous distribution functions, so that in this case a unique decomposition of any multivariate distribution into its one-dimensional marginal distributions and a copula function C exists (Sklar, 1959). Throughout the paper the marginal distributions are assumed to be known, hence the marginal distributions can be treated as uniformly distributed by the probability integral transform.

A subclass of copulas that recently is in the focus of general interest are the vine copulas, which is a decomposition of a p-dimensional probability distribution into $p(p-1)/2$ bivariate conditional and unconditional copula functions (Joe, 1996, 1997; Bedford and Cooke, 2001, 2002; Czado, 2010). Each of these bivariate copula functions needs to be fitted to the respective marginal distributions from the sample. Since the mere number of available bivariate copulas classes is endless and the computational effort is considerably high especially for large p, it is advantageous to not consider every available copula in the fitting process. Additionally, using inappropriate copula models by neglecting asymmetries in the data can lead to incorrect conclusions, see Krupskii (2016). Thus, by testing for symmetry, copulas can be eliminated that do not have suitable symmetry properties to properly describe the data. So it is necessary to know which concepts of symmetry could be present (see Klein and Fischer (2004) for a general overview). In applications for example, where especially the multivariate lower or upper tail is of importance, it is advisable to analyze the tail dependence of both tails and test for differences (Joe, 1993; Hua and Joe, 2011).

This paper introduces two new concepts of symmetry for bivariate copulas ($\mathbf{X}$ and $\mathbf{Y}$) with main focus on the tails which are located at the vertices of the unit square. Two testing

procedures for detecting deviations from the new symmetry concepts and implicitly radial symmetry are provided. Additionally, the involved test statistic enables to measure and test for asymmetries in the tails of a distributions. Throughout this paper, only the bivariate case is discussed, which is common in literature focusing symmetry concepts of copulas. However, due to the intuitive geometric interpretation, a generalization of $\mathbf{X}$, $\mathbf{Y}$, and their respective statistical tests to higher dimensions is straightforward.

This paper is organized as follows: Section 2 starts by briefly providing an overview on established symmetry concepts for bivariate copulas. Two new symmetry concepts with main focus on the tails of the copula are defined and relations to existing concepts are identified. Section 3 lists non- and semiparametric testing procedures for existing symmetries from recent literature and proposes tests for $\mathbf{X}$ and $\mathbf{Y}$ together with the required preliminaries following Mangold (2015). In section 4, size and power of the newly derived tests are analyzed by comparison to existing state-of-the-art tests of Genest and Nešlehová (2014) and Krupskii (2016) via Monte Carlo simulation. Section 5 showcases the flexibility of the new tests by an application to a dataset and within the vine copula fitting process. Section 6 summarizes and shows further opportunities of extensions of the new concepts.

2. Symmetry concepts for bivariate copulas

The functional symmetry concepts $\mathbf{J}$, $\mathbf{R}$, $\mathbf{E}$, $\mathbf{X}$, and $\mathbf{Y}$ are introduced for bivariate copulas in this section. A copula is defined as follows:

Definition 1 (Copula, Nelsen (2006)). *A function $C : [0,1]^p \mapsto [0,1]$ is a p-dimensional copula if*

- $C(u_1, \ldots, u_{i-1}, 0, u_{i+1}, \ldots, u_p) = 0$: *If at least one argument $u_i = 0$, then the value of C is 0, $i = 1, ..., p$.*

- $C(1, \ldots, 1, u_i, 1, \ldots, 1) = u_i$: *If all arguments are equal to 1 except for u_i, C is a distribution function of the uniform distribution, $i = 1, ..., p$.*

- *C is p-non-decreasing: For every $H = \prod_{i=1}^{p}[x_i, y_i] \subseteq [0,1]^p$, the integral*

$$\int_H \mathrm{d}C(\boldsymbol{u}) \geq 0$$

3

for $\boldsymbol{u} = (u_1, ... u_p)' \in [0, 1]^p$ with respect to C. The copula density function is denoted as c.

2.1. Established symmetry concepts

Although there are many more symmetry concepts for distributions in general (see Nelsen (1993)), there are three main concepts for copulas, $\mathbf{J}$, $\mathbf{R}$, and $\mathbf{E}$, that are defined in the following:

Definition 2 (Joint symmetry, Nelsen (1993))**.** *A copula C is joint symmetric ($\boldsymbol{J}$) if and only if*

$$C(u, v) = u - C(u, 1 - v) \ \text{ and } \ C(u, v) = v - C(1 - u, v), \tag{1}$$

$u, v \in [0, 1]$.

A more general concept is the radial symmetry, if the copula function is identical to the survival copula $\bar{C}(u, v) = C(1 - u, 1 - v) + u + v - 1$:

Definition 3 (Radial symmetry, Nelsen (1993))**.** *A copula C is radially symmetric ($\boldsymbol{R}$) if and only if*

$$C(u, v) = C(1 - u, 1 - v) + u + v - 1 = \bar{C}(u, v), \tag{2}$$

$u, v \in [0, 1]$.

Note that every joint symmetric copula is also radially symmetric ($\mathbf{J} \rightarrow \mathbf{R}$), while the opposite is not true in general (Nelsen, 1993). A third concept is discussed in the context of meta-elliptical distributions (Fang et al., 2002): the concept of exchange symmetry, or also called permutation symmetry.

Definition 4 (Exchange symmetry, Genest et al. (2012) – Permutation symmetry (Krupskii, 2016))**.** *A copula C is exchange/permutation symmetric ($\boldsymbol{E}$) if and only if*

$$C(u, v) = C(v, u), \tag{3}$$

$u, v \in [0, 1]$.

2.2. New symmetry concepts

The following analysis focuses on the vertices of $[0,1]^p$. As simplification, a notation for vertices is introduced: Let $\boldsymbol{v}$ be a vertex of $[0,1]^p$, $\boldsymbol{v} = (v_1, v_2, ..., v_p)'$, $v_j \in \{0,1\}, j = 1, ..., p$. A unique identifier of $\boldsymbol{v}$ can be obtained by calculating the decimal value of the binary number $v_1 v_2 \cdots v_p$ and adding 1 (as example, the three-dimensional vertex $(1,1,0)'$ has the number 7, since $110_2 = 6_{10}$ augmented by one equals 7). Main focus of this article are bivariate square-shaped regions with edge length c, located at each corner of $[0,1]^2$ (see figure 1). The probabilities of observing a realization from those regions needs to coincide in the following manner:

Definition 5 (Vertex symmetry). *A copula C is called vertex symmetric ($\boldsymbol{X}$) if the probability of an observation within a square of side length c located at each vertex of $[0,1]^2$ is equally likely:*

$$C(c,c) = c - C(1-c, c) = c - C(c, 1-c) = C(1-c, 1-c) + 2c - 1, \qquad \text{for } 0 < c < \frac{1}{2}.$$

A copula C is called c'-vertex symmetric ($\boldsymbol{X}_{c'}$), if C is vertex symmetric for all c, $0 < c \leq c' < \frac{1}{2}$.
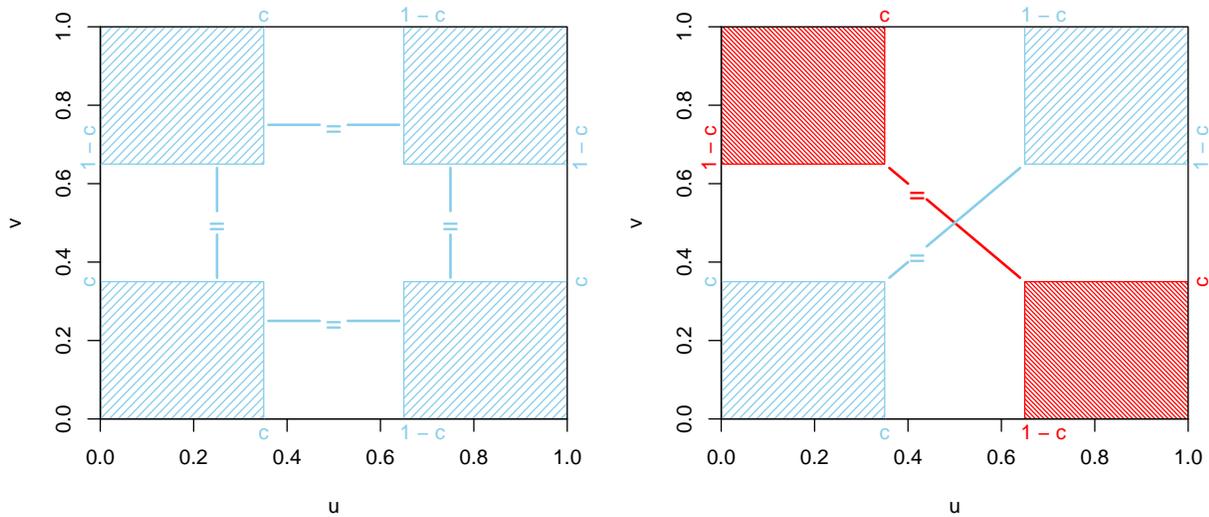

Figure 1: Schematic representation of the symmetry concepts $\boldsymbol{X}$ (left) and $\boldsymbol{Y}$ (right) for $c = 0.35$.

Figure 1 (left) provides a sketch of the concept of vertex symmetry. A weaker concept of symmetry is provided by the next definition:

Definition 6 (Diametrical symmetry). *A copula C is called diametrically symmetric ($\mathbf{Y}$) if occurrences of realizations are equally likely in areas around vertices that are on the diametrically opposed side of $[0,1]^2$:*

$$C(c,c) = C(1-c, 1-c) + 2c - 1 \;\; and \;\; C(c, 1-c) = C(1-c, c), qquad for \; 0 < c < \frac{1}{2}.$$

A copula C is called c'-diametrically symmetric ($\mathbf{Y}_{c'}$), if C is diametrically symmetric for all c, $0 < c \le c' < \frac{1}{2}$.

Again, a sketch of the concept of diametrical symmetry can be found in figure 1 (right).

Note that this concepts with the focus on the vertices of $[0,1]^2$ can easily be extended to arbitrary dimensions p which is described in section 6 but omitted here for the sake of simplicity. There is a connection between the two new symmetry concepts $\mathbf{X}$ and $\mathbf{Y}$:

Remark 1. *If a copula is vertex symmetric, it is also diametrically symmetric, $\mathbf{X} \to \mathbf{Y}$. The opposite is not true in general.*

Remark 2. *As a consequence of remark 1, only one out of three situations can occur: a copula has both, $\mathbf{X}$ and $\mathbf{Y}$, has $\mathbf{Y}$ only, or has neither $\mathbf{X}$ nor $\mathbf{Y}$. For the first case, examples are the independence copula and a copula with distribution function*

$$C(u,v) = u\,v\,(2\,(u^2 + v^2) - 3\,(u+v) + 3), \tag{4}$$

which is a scaled twodimensional parabola centered at the point $(0.5, 0.5)'$. The FGM-copula (Farlie, 1960; Gumbel, 1960; Morgenstern, 1956) and the copula of Fréchet (1958) are examples of the second case. Examples for the third case are the Clayton (Clayton, 1978) and the Gumbel copula (Gumbel, 1960; Barnett, 1980) together with any other non-radially symmetric copula family as will be shown in the following.

The parameter c defines the zones of $[0,1]^2$ that are in focus of the property $\mathbf{X}$ and $\mathbf{Y}$. Choosing c close to 0.5 divides $[0,1]^2$ into four mutually exclusive parts covering almost the entire unit square. The smaller c, the more the symmetry definitions are focused on the tail

behavior of the copula C. Comparing heaviness of multivariate tails can be of interest in many applications, especially in absence of tail dependence or if multivariate skewness in the tails needs to be modeled. Convenient values of c and resulting implications are discussed in section 3.2.

Next, the new symmetry concepts $\mathbf{X}$ and $\mathbf{Y}$ are incorporated into the existing framework of $\mathbf{J}$, $\mathbf{R}$, and $\mathbf{E}$. Nelsen (1993) provided an overview of the different combinations of the symmetry concepts $\mathbf{J}$, $\mathbf{R}$, and $\mathbf{E}$ and illustrated one distribution from each combination. He identified in total 14 different possible constellations[2] – 6 of those constellations are of interest in the present context (see figure 6 in the appendix for scatter plots of the relevant distributions from Nelsen (1993)). This restriction arises from omitting two concepts that cannot be transmitted to copulas. The remaining 6 constellations of $\mathbf{J}$, $\mathbf{R}$, and $\mathbf{E}$ are listed in table 1.

Table 1: List of distributions covering all possible constellations of symmetry concepts $\mathbf{J}$, $\mathbf{R}$, and $\mathbf{E}$ from Nelsen (1993), along with new concepts $\mathbf{X}$ and $\mathbf{Y}$. There are three possible constellations: $\mathbf{X}$ and $\mathbf{Y}$, $\mathbf{Y}$ only, and neither $\mathbf{X}$ nor $\mathbf{Y}$. A checkmarked cell indicates that the row's distribution has the symmetry concept denoted by the respective column. Missing numbers of the first column are caused by duplettes in Nelsen (1993) regarding $\mathbf{J}$, $\mathbf{R}$, and $\mathbf{E}$. Examples for the distributions are presented in figure 6 in the appendix.

Nr. of. distr.	J	R	E	X & Y	Y	-
				Symmetry concepts		
1	✓	✓	✓	✓		
3			✓			✓
4	✓	✓		✓		
6						✓
8		✓	✓		✓	
11		✓		✓		

By examining the squared regions close to the four vertices $(0,0)'$, $(0,1)'$, $(1,0)'$, and $(1,1)'$ it is to decide whether the respective constellation inherits $\mathbf{X}$ and/or $\mathbf{Y}$ by strictly applying definitions 5 and 6. Analyzing the distributions of table 1, three scenarios can be

---

[2]See figure 1 in Nelsen (1993).

identified: Occurrence of **X** and **Y** as first, **Y** but not **X** as second, and neither **X** nor **Y** as the third case. Since table 1 captures all possible combinations of the concepts **J**, **R**, and **E**, the following three conclusions can be drawn: First, from the existence of **X** and **Y** the existence of **R**. Second, from the existence of **Y** only the existence of **R** together with **E**. Third, from the absence of **X** and **Y** the absence of **R** (and simultaneously of **J**). As a consequence, a test for **Y** can also be used to test for radial symmetry, which is discussed section 3.2.

3. Testing for bivariate symmetry

This section gives an overview on state-of-the-art tests for the symmetry concepts of section 2.1 and provides rank-based tests for the new symmetry concepts of section 2.2. In line with recent literature concerning nonparametric test for symmetry, this paper introduces and discusses the bivariate case only. However, the underlying measure of Mangold (2015) has originally been developed for arbitrary dimensions p. Thus, the proposed concepts can easily be extended to dimensions $p > 2$ as pointed out in section 6.

3.1. Overview on tests for established symmetry concepts

The symmetry concept **J** has been focus of research of Li and Genton (2013), which resulted in a nonparametric test for joint symmetry based on the empirical copula process that tests for differences in the empirical version of equation (1). The asymptotic distribution of the test statistic is obtained using bootstrap. Recently, many researchers interest was on radial symmetry (**R**), see Hua and Joe (2011), Li and Genton (2013), Rosco and Joe (2013), Genest and Nešlehová (2014), and Krupskii (2016) who introduced various non- and semiparametric testing procedures as a Cramér-von-Mises-type test based on differences in equation (2). Again, the asymptotic distribution contains Brownian bridges which requires resampling techniques for determining critical values. Tests for exchange symmetry (**E**) have been proposed by Genest et al. (2012), Li and Genton (2013), and Krupskii (2016), who examine the performance of the respective test using a Monte-Carlo simulation.

Next, two test statistics that allow hypothesis testing for the newly introduced kinds of symmetry are introduced.

3.2. Tests for new symmetry concepts

First, some basic ideas and definitions are presented that are needed in order to test for the new concepts of symmetry **X** and **Y**, starting with a new generalization of the bivariate FGM copula:

Definition 7 (Bivariate polynomial copula, Mangold (2015))**.** *Bivariate polynomial copulas with parameter $\alpha > 0$ and $\boldsymbol{\theta} = (\theta_1, \theta_2, \theta_3, \theta_4)' \in \Theta \subset \mathbb{R}^4$ have the distribution function*

$$C_{\boldsymbol{\theta}}^{\alpha} = C_{(\theta_1, \theta_2, \theta_3, \theta_4)'}^{\alpha}(u, v) = uv \left(1 + (1 - u)(1 - v) \right.$$
$$\times \left[((1 - u)(1 - v))^{\alpha} \theta_1 + ((1 - u)v)^{\alpha} \theta_2 + (u(1 - v))^{\alpha} \theta_3 + (uv)^{\alpha} \theta_4 \right] \right),$$

for $u, v \in [0, 1]$. The density function of the polynomial copula is denoted as $c_{\boldsymbol{\theta}}^{\alpha}$.

Figure 2 displays two density functions of the polynomial copula for different values of α.
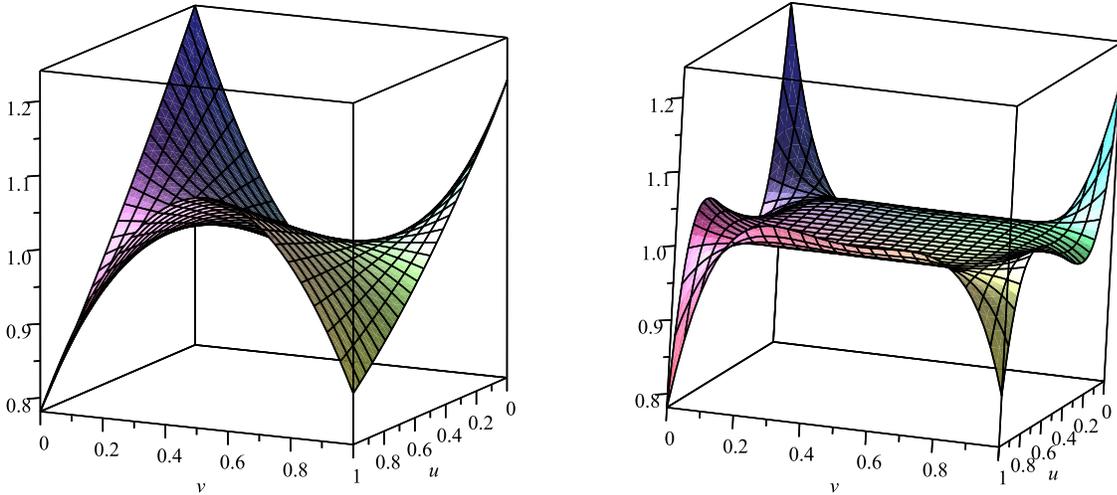
Figure 2: Left: Density function of the copula by Nelsen et al. (1997), which is a special case of the polynomial copula ($\alpha = 1$). Right: Density function of the polynomial copula for $\alpha = 5$. Both copulas have a parameter vector $\boldsymbol{\theta} = (-0.15, 0.22, -0.18, 0.24)'$.

However, not every vector $\boldsymbol{\theta} \in \mathbb{R}^4$ results in a proper copula according to definition 1 – see Mangold (2015) for an explicit parameter space Θ if $\alpha = 1$. Unfortunately, there is no

closed form expression of Θ for $\alpha \neq 1$. However, for the purpose of this article, the following lemma is sufficient:

Lemma 1 (Admissibility). *For every $0 < \alpha < \infty$, there exists an $\epsilon > 0$ such that $\boldsymbol{\theta} \in [-\epsilon, \epsilon]^4$ is admissible and $C_{\boldsymbol{\theta}}^{\alpha}$ is a copula function according to definition 1.*

Proof. Follows directly from the uniform continuity of polynomials on a closed interval $[0, 1]$, since $\boldsymbol{\theta} = (0, 0, 0, 0)'$ is admissible, since it results in the independence copula (see proposition 1 in Mangold (2015)). $\qquad \square$

The family of polynomial copulas contains well-known copulas as special cases (for example the bivariate copula with cubic sections from Nelsen et al. (1997) for $\alpha = 1$, see figure 2). One particular property of polynomial copulas from definition 7 is that for every value of $\alpha > 0$, the density function $c_{\boldsymbol{\theta}}^{\alpha}$, evaluated at the vertices of $[0, 1]^2$, is

$$c_{\boldsymbol{\theta}}^{\alpha}(0,0) = 1 + \theta_1 \qquad c_{\boldsymbol{\theta}}^{\alpha}(0,1) = 1 - \theta_2 \qquad c_{\boldsymbol{\theta}}^{\alpha}(1,0) = 1 - \theta_3 \qquad c_{\boldsymbol{\theta}}^{\alpha}(1,1) = 1 + \theta_4. \quad (5)$$

Concisely, each parameter corresponds to exactly one vertex. The parameter α does not affect the value in the vertices, only the shape of the density function. The higher α, the closer to 1 is the density of the copula at the center of $[0, 1]^2$ and the steeper is it in regions close to the vertices. Since the density function of the independence copula is 1 for all $u, v \in [0, 1]$, $\boldsymbol{\theta}$ contains information on deviations from independence in areas close to the vertices. However, due to the curse of dimensionality and restrictions concerning the feasibility of $\boldsymbol{\theta}$, one cannot simply estimate $\boldsymbol{\theta}$ of the polynomial copula from definition 7 using maximum likelihood or kernel density estimation in higher dimensions as discussed in Mangold (2015). Instead, Mangold (2015) introduces an alternative method to deduct information on $\boldsymbol{\theta}$ from a test statistic of a test for independence, introduced in the next proposition 1. This new method extends the basic procedure of determining the locally most powerful rank tests for independence (LMPRT, see Garralda-Guillén (1998); Genest and Verret (2005) for the bivariate case) to the p-variate, multiparametric setting following Mangold (2015). The resulting test statistic, when applied to the polynomial copula, then contains all LMPRT statistics related to every vertex of the unit cube $[0, 1]^p$:

Proposition 1 (Mangold (2015)). *Let $(R_{1i}, ..., R_{ji}, ..., R_{pi})'$, $i = 1, ..., n$, $j = 1, ..., p$, be the ranks associated to a p-dimensional i.i.d sample of size n from a population with copula function C_θ, $\theta \in \mathbb{R}$. Under assumptions A1–A4 (see Mangold (2015)), T_n^* is a locally most powerful rank test (LMPRT) for $H_0 : \theta = 0$,*

$$T_n^* = \frac{1}{n} \sum_{i=1}^n T(R_{1i}, ..., R_{ji}, ..., R_{pi})$$

with

$$T(r_1, ..., r_j, ..., r_p) = \mathbb{E}\left[\frac{\partial}{\partial \theta} \log c_\theta(\boldsymbol{B}) \bigg|_{\theta = \theta_0} \right],$$

$\boldsymbol{B} = (B_{r_1}, ..., B_{r_j}, ..., B_{r_p})'$ *containing independently beta distributed random variables* $B_{r_j} \sim \beta(r_j, n - r_j + 1)$, $j = 1, ..., p$. *If H_0 is true and assumptions A5 and A6 (see Mangold (2015)) are met, then*

$$\sqrt{n}T_n^* \overset{asy}{\to} \mathcal{N}(\theta_0, \sigma^2(\dot{c}_{\theta_0})), \qquad with \ \sigma^2(\dot{c}_{\theta_0}) = \int_{(0,1)^p} |\dot{c}_{\theta_0}(\boldsymbol{u})|^2 \, \mathrm{d}u.$$

Let $C_{\boldsymbol{\theta}}$ be a p-dimensional, q-parametric copula, $\boldsymbol{\theta} \subseteq \mathbb{R}^q$ where $\boldsymbol{\theta} = (0, ..., 0)'$ if and only if $C_{\boldsymbol{\theta}}$ is the independence copula. Then, the q-dimensional vector

$$\boldsymbol{T} = \mathbb{E}\left[\frac{\partial}{\partial \boldsymbol{\theta}} \log c_{\boldsymbol{\theta}}(\boldsymbol{B}) \bigg|_{\boldsymbol{\theta} = \boldsymbol{\theta}_0} \right]$$

contains all LMPRT statistics for $\theta_{[k]} = (0, 0, ..., 0, \theta_k, 0, ..., 0)'$, $k = 1, ..., q$. $\boldsymbol{T}$ is asymptotically normal distributed with $\boldsymbol{\mu} = \boldsymbol{0}$ and $\Sigma(\dot{c}_{\boldsymbol{0}})$, where

$$\Sigma(\dot{c}_{\boldsymbol{0}})_{i,j} = \int_{[0,1]^p} \left(\frac{\partial c_{\boldsymbol{\theta}}(\boldsymbol{u})}{\partial \theta_i} \bigg|_{\boldsymbol{\theta} = \boldsymbol{0}} \right) \times \left(\frac{\partial c_{\boldsymbol{\theta}}(\boldsymbol{u})}{\partial \theta_j} \bigg|_{\boldsymbol{\theta} = \boldsymbol{0}} \right) d\boldsymbol{u} \ for \ i, j = 1, ..., q.$$

The realization of $\boldsymbol{T}$ is denoted as $\boldsymbol{t}$, single components of $\boldsymbol{T}$ ($\boldsymbol{t}$) as T_j (t_j), $j = 1, ..., q$.

Proof. See Mangold (2015). $\qquad\qquad\qquad\qquad\qquad\qquad\qquad\qquad\qquad\qquad\qquad$ □

Remark 3. *A Cholesky decomposition $\boldsymbol{L}$ of $\Sigma(\dot{c}_{\boldsymbol{0}})^{-1}$ transforms $\boldsymbol{T}$ into its scaled version $\boldsymbol{T}^s := \boldsymbol{L}'\boldsymbol{T}$.*

The reduced form of the bivariate family of polynomial copulas from definition 7 (see Mangold (2015) for the general definition for p dimensions) satisfies the assumptions A1–A6;

therefore the proposition 1 can be applied, which results in the test statistic $\boldsymbol{T}_\alpha$. Note that for $\boldsymbol{\theta} = (0,0,0,0)'$, the independence copula is uniquely nested in the polynomial copula for every $\alpha > 0$ (see proposition 1 in Mangold (2015)). Conclusions from $\boldsymbol{T}_\alpha$ on $\boldsymbol{\theta}$ can be achieved by analyzing the sign of the realization $\boldsymbol{t}_\alpha$, since $\mathbb{E}[\boldsymbol{T}_\alpha] = \boldsymbol{\theta}_0 = (0,0,0,0)'$ under the Null hypothesis of independence according to proposition 1. For example, a positive sign of the first entry of $\boldsymbol{t}_\alpha$ implies a higher probability for an observation occurring in an area $[0, \epsilon]^2$ which is close to the vertex $\boldsymbol{v}_1$ for small $\epsilon > 0$ than in the case of independence, and a negative sign for a lower probability. As a downside however, $\boldsymbol{t}_\alpha$ cannot be interpreted as vector of estimates for the parameters of the polynomial copula anymore, but rather as a descriptive measure for signed deviations from the density function of the independence copula evaluated in regions close to the vertices of $[0, 1]^2$. Knowing the asymptotic distribution of $\boldsymbol{T}_\alpha$ allows both, creating confidence bands for single components of $\boldsymbol{t}_\alpha$ to detect deviations from zero and testing for joint differences of deviations from independence over all vertices. The first can be used to order tails by thickness by directly comparing deviations from independence in vertices, the latter is extended to a test of independence based on the joint deviation from zero, see Mangold (2015).

In the bivariate case, one could be interested in discussing differences in the tails associated to $(0, 0)'$ and $(1, 1)'$, to decide whether the tails are equally heavy or not. Equally heavy tails would result in identical deviations from independence in regions close to the vertices $\boldsymbol{v}_1$ and $\boldsymbol{v}_4$. Most of statistical measures for tail symmetry (or symmetry of tail dependence) are neglecting potential asymmetries in the remaining two vertices $(0, 1)'$ and $(1, 0)'$. Additional asymmetries in those vertices require specific copula families and can now be identified comparing the second and third entry of $\boldsymbol{t}_\alpha$. The occurrence of certain patterns in the tails can also be used in order to choose from a set of feasible distribution families for modeling dependence, which is further addressed in section 5.2. Note that only asymmetries in tails, not asymmetry in tail dependence can be detected using $\boldsymbol{T}_\alpha$, since polynomial copulas themselves cannot model tail dependency (see Nelsen (2006)).

Remark 4. *For small c, a vertex symmetric copula is equivalent to a copula where deviations from the density of the independence copula are identical within a square of side length c located at every vertex. The last statement is also true for diametrical symmetric copulas*

12

and vertices that are located diametrically opposed in $[0, 1]^2$.

$\boldsymbol{T}_\alpha^s$, the scaled version of $\boldsymbol{T}_\alpha$, is now used to test for symmetry under the alternative of vertex and/or diametrical symmetry from section 2.2 and thus implicitly under the alternative of radial symmetry.

Corollary 1 (Test for vertex symmetry). *For a fixed value c, $0 < c < \frac{1}{2}$, the pair of hypotheses*

$$H_0 : \text{ Vertex symmetry} \qquad H_A : \text{ No vertex symmetry}$$

can be tested using $\boldsymbol{T}_\alpha^s$, the scaled statistic of proposition 1 applied to polynomial copulas, since under H_0

$$T_\alpha^X = \frac{1}{2} \left(\boldsymbol{R}^X \boldsymbol{T}_\alpha^s \right)' \left(\boldsymbol{R}^X \boldsymbol{T}_\alpha^s \right) \overset{asy}{\sim} \chi^2(3), \qquad with \; \boldsymbol{R}^X = \begin{pmatrix} 1 & 1 & 0 & 0 \\ 0 & 1 & -1 & 0 \\ 0 & 0 & 1 & 1 \end{pmatrix}.$$

H_0 needs to be rejected if T_α^X exceeds a threshold of the χ^2-distribution with 3 degrees of freedom, corresponding to the level of the test.

Proof. If H_0 is true, expected deviations from independence are identical in each vertex. Thus, using the scaled realization $\boldsymbol{t}_\alpha^s$ as a descriptive measure for deviation from independence, we expect $t_{\alpha,1}^s \approx -t_{\alpha,2}^s \approx -t_{\alpha,3}^s \approx t_{\alpha,4}^s$, or $t_{\alpha,1}^s \approx -t_{\alpha,2}^s$, $t_{\alpha,2}^s \approx t_{\alpha,3}^s$, and $-t_{\alpha,3}^s \approx t_{\alpha,4}^s$ under the Null. The signs need to be added to $T_{\alpha,i}^s$ considering equation (5), such that $T_{\alpha,i}^s > 0$ results in a greater probability than under independence, $i = 1, ..., 4$. By proposition 1, $\boldsymbol{T}_\alpha^s$ is asymptotically standard normal distributed. Therefore, the difference of two components follows $\mathcal{N}(\mu = 0, \sigma = \sqrt{2})$. The sum of the three standardized squared differences follows asymptotically a χ^2 distribution with 3 degrees of freedom. $\square$

Corollary 2 (Test for diametrical symmetry). *For a fixed value c, $0 < c < \frac{1}{2}$, the pair of hypotheses*

$$H_0 : \text{ Diametrical symmetry} \qquad H_A : \text{ No diametrical symmetry}$$

can be tested using $\boldsymbol{T}_\alpha^s$, the scaled statistic of proposition 1 applied to polynomial copulas, since under H_0

$$T_\alpha^Y = \frac{1}{2}\left(\boldsymbol{R}^Y \boldsymbol{T}_\alpha^s\right)'\left(\boldsymbol{R}^Y \boldsymbol{T}_\alpha^s\right) \overset{asy}{\sim} \chi^2\left(2\right), \qquad with\ \boldsymbol{R}^Y = \begin{pmatrix} 1 & 0 & 0 & -1 \\ 0 & 1 & -1 & 0 \end{pmatrix}.$$

H_0 needs to be rejected if T_α^Y exceeds a threshold of the χ^2-distribution with 2 degrees of freedom, corresponding to the level of the test.

Proof. If H_0 is true, expected deviations from independence are identical in each diametrically opposed vertex. Again, using the scaled realization $\boldsymbol{t}_\alpha^s$ as a descriptive measure for deviation from independence, we expect $t_{\alpha,1}^s \approx t_{\alpha,4}^s$ and $t_{\alpha,2}^s \approx t_{\alpha,3}^s$ under the Null. By proposition 1, $\boldsymbol{T}_\alpha^s$ is asymptotically standard normal distributed. Therefore, the difference of two components follows $\mathcal{N}(\mu = 0, \sigma = \sqrt{2})$. The sum of the two standardized squared differences follows asymptotically a χ^2 distribution with 2 degrees of freedom. $\qquad\square$

Remark 5. *If one wants to test for $\boldsymbol{X}_{c'}$ or $\boldsymbol{Y}_{c'}$, the equations of definition 5 and 6 must hold for all values c below the threshold c', $0 < c' < \frac{1}{2}$. Thus, testing for c'-vertex and c'-diametrical symmetry implies testing for a sequence of values $0 < c_1 < ... < c_m \leq c'$ using the tests of the corollaries 1 and 2. If H_0 cannot be rejected for neither of the c_k, $k = 1,...,m$, the Null hypothesis of c'-diametrical or c'-vertex symmetry cannot be rejected either.*

Corollary 3 (Test for radial symmetry)**.** *Testing the pair of hypotheses of corollary 2 results in a test for radial symmetry, described by the hypotheses*

$$H_0: \quad Bivariate\ radial\ symmetry \qquad H_A: \quad No\ bivariate\ radial\ symmetry.$$

H_0 is rejected, if the Null hypotheses of corollary 2 is rejected at a prespecified level of error.

Proof. The rejection of radial symmetry if diametrical symmetry is rejected follows immediately from the relations between the concepts described in section 2.2. Inserting $C(c,c)$ and $C(c, 1-c)$ into the definition of radial symmetry results in the equations of definition 6. $\quad\square$

Recall that the polynomial copula family $C_{\boldsymbol{\theta}}^\alpha$ has a nuisance parameter α. The higher α, the longer the density function remains close to the value of 1 as one approaches the vertices (see figure 2). α needs to be determined before any of the testing procedure is applied.

For practical purposes, a rule of thumb is supplied for a connection between the nuisance parameter α of the tests and the value c of the symmetry concepts. It is based on sensitive regions of the influence function (IF) of $\boldsymbol{T}_\alpha$, following Hampel (1986). The IF is a Gâteaux derivative and measures the impact of a small contamination in a sample on a statistical functional.

At first using a simulation, later explicitly, the impact of changes in a bivariate sample at a point $(u, v)'$, $u, v \in [0, 1]$, on $\boldsymbol{T}_\alpha$ is analyzed to gain a better insight into the sensitive regions of $\boldsymbol{T}_\alpha$. To avoid redundancy, this analysis has only been carried out for $T_{\alpha,1}$, the first element of $\boldsymbol{T}_\alpha$. In the following simulation, a sample size of $n = 100$ is chosen; the results are stable for smaller or larger sample sizes. First, $N = 5{,}000$ samples from the independence copula are drawn and $T_{\alpha,1}$ is calculated for each sample for different values of α. Second, the first observation $(u_1, v_1)'$ of each sample is consecutively replaced by a distorting observation $(u_1', v_1')'$ from a grid of $[0, 1]^2$ containing 100×100 values. Third, $T_{\alpha,1}'$ is calculated for each of the 10,000 distorted samples and the differences between $T_{\alpha,1}'$ and $T_{\alpha,1}$ are arranged in a matrix, again for different values of α. Finally, the 5,000 resulting 100×100 matrices are averaged componentwise to obtain a simulated influence curve as shown in figure 3.

Table 2: Position c^* of the cross-shaped transition border from figure 3 for different α and values of an approximating function $(\alpha + 2)^{-1}$.

	α							
	0.5	1	2	3	4	10	25	100
c^*	0.42	0.36	0.27	0.22	0.18	0.09	0.04	0.01
$(\alpha + 2)^{-1}$	0.40	0.33	0.25	0.20	0.17	0.08	0.04	0.01

There is an area where the functional $T_{\alpha,1}$ reacts sensitive on changes in the sample. This area is located in a square containing the vertex $(0, 0)$ as expected. Interestingly, there seems to be a cross-shaped transition border that separates this sensitive area from zones where a change in an observation results in a negative influence on the value of $T_{\alpha,1}$. Table 2 reports the position c^* of this transition border for several values of α together with a proposal for an approximating function $(\alpha + 2)^{-1}$.

Since the test statistics of the corollaries 1 and 2 require a fixed value c, it is convenient
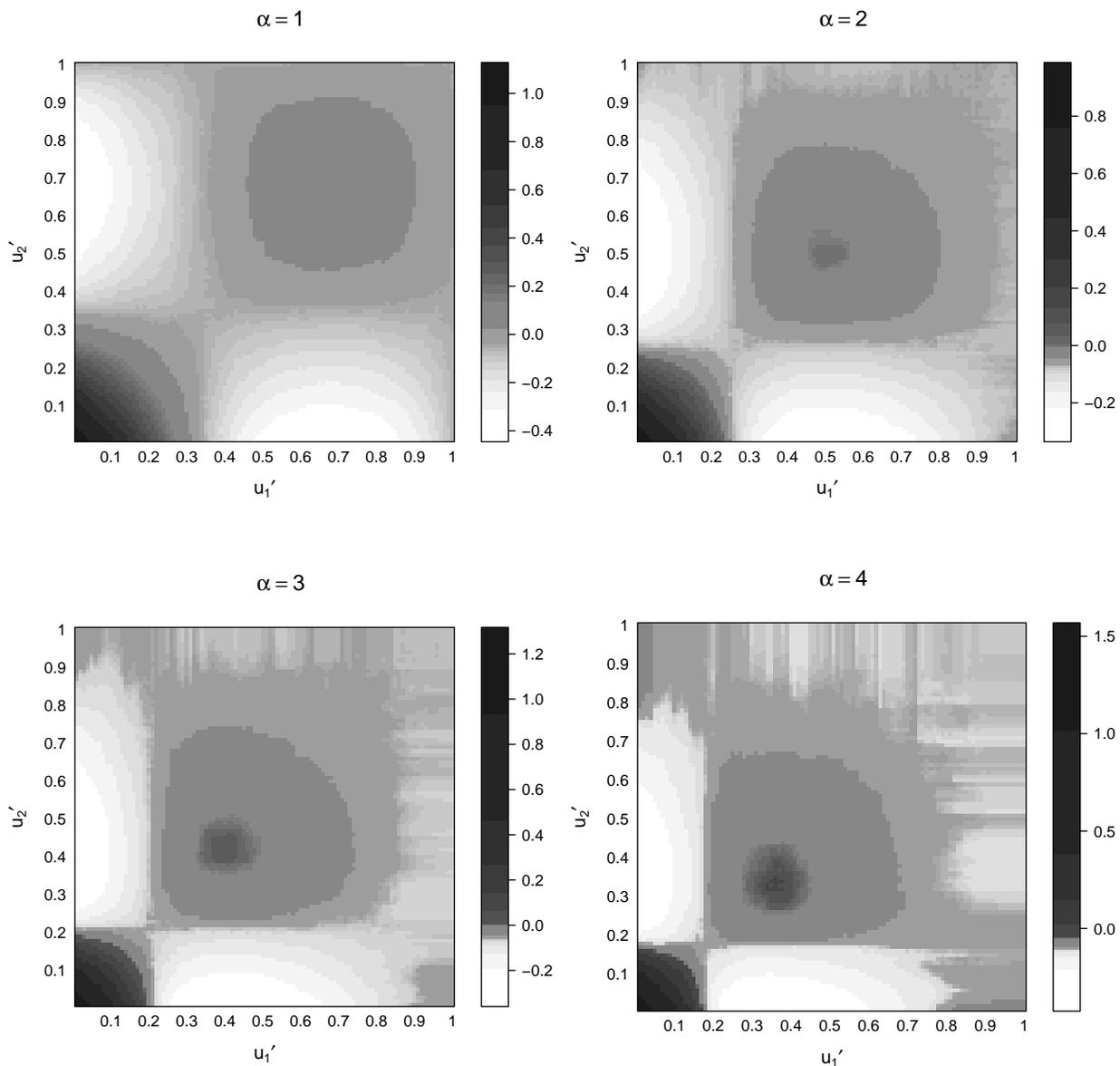
Figure 3: Simulated influence functions of $T_{\alpha,1}$ for $\alpha = 1, 2, 3, 4$ and sample size $n = 100$. The most sensitive area is located at the vertex $(0, 0)$, the sensitivity increases with augmenting α. The cross-shaped transition border from white (negative impact) to dark tinted areas (positive impact) changes, as α varies.

to choose $c = c^*$ such that the regions of interest in $[0, 1]^2$ coincide with the sensitive regions of $T_{\alpha,1}$. Hence, α can be chosen for calibration given a value of c and vice versa. Note that using the approximation $(\alpha + 2)^{-1}$, the requirement $0 < c < \frac{1}{2}$ from definitions 5 and 6 changes to $\alpha > 0$, which is always true by definition 7.

In the classical extreme value theory, the region that is considered as tail of a distribution is located below (above) a certain threshold which is often given by a quantile. Thus, in situations where the symmetry in tails is of special interest and shall be tested using T_α^X and T_α^Y, c could take on values as $0.1, 0.05$ or 0.01. This can be achieved by an α of 8, 18 and 88, if the approximation from table 2 is used. Note that the sensitive regions for small c are very narrow; as in extreme value theory, a sufficiently large sample size is required to assure observations within those regions.

Interestingly, the vector $\boldsymbol{T}$ from proposition 1 is identically to a vector of test statistics $\boldsymbol{T}^M$ resulting from a Lagrange-multiplier approach. Since $\boldsymbol{T}^M$ can be embedded into the framework of M-estimators, the influence function of its components, e.g. for the first component, is proportional to

$$\frac{\partial}{\partial \theta_1} \left[\log c_{(\theta_1,0,0,0)'}(u,v) \right]_{\theta_1=0}.$$

Solving the latter equation for $(u,v)'$ leads to $((\alpha+2)^{-1}, (\alpha+2)^{-1})'$, which coincides with the proposed function in table 2. Thus, setting $c^* = (\alpha+2)^{-1}$ ensures that only observations close to the vertex $(0,0)'$ that are located within the square with length c^* have a strong and positive effect on the first component of $\boldsymbol{T}$ and thus on T_α^X and T_α^Y.

Finally, it shall be pointed out that alternatively the concepts $\mathbf{X}$ and $\mathbf{Y}$ could be tested using a Cramér-von-Mises-type test statistic, using the average squared difference of the equations in definition 5 and 6 based on an empirical copula process for all $c \in [0, 0.5]$. However, the computational restrictions are very high for large sample sizes and/or large dimensions, since the amount of equations is affected exponentially by augmenting dimension p. A more detailed research will be subject to further investigation.

4. Simulation studies

In this section, applications of the introduced tests for the symmetry concepts $\mathbf{X}$ and $\mathbf{Y}$ are presented. Since this paper has a practice oriented focus, the majority of the presented simulations are carried out with respect to radial symmetry. The results are compared to other recently published nonparametric tests for radial symmetry (Li and Genton, 2013;

Genest and Nešlehová, 2014; Krupskii, 2016). Throughout the following sections, the level of error is fixed at 5%.

4.1. Detecting radial symmetry in distributions of Nelsen (1993)

Nelsen itemized several non-standard distributions each representing a combination of the symmetry concepts of table 1, together with two other symmetries that are not focused in this article. In this section, the test of corollary 3 is used to identify distributions without the property **R**. Table 3 shows rejection rates for distributions with the combination of symmetries from table 1, based on 1,000 samples of different sample sizes n and values of α.

Table 3: Simulated rejection rates for the distributions from table 1 in percent, based on 1,000 samples of size n for $\alpha = 1, 2, 3$. Distributions 3 and 6 are not radially symmetric.

Distr.	$n = 100$			$n = 250$			$n = 1{,}000$		
	$\alpha = 1$	$\alpha = 2$	$\alpha = 3$	$\alpha = 1$	$\alpha = 2$	$\alpha = 3$	$\alpha = 1$	$\alpha = 2$	$\alpha = 3$
1	26.5	4.9	3.6	43.7	10.5	10.9	90.1	63.4	57.0
3	100	77.8	20.8	100	99.7	63.0	100	100	100
4	10.8	5.6	3.1	17.8	9.1	8.9	39.6	17.5	23.1
6	100	100.0	73.4	100	100	99.9	100	100	100
8	4.4	5.2	5.6	15.1	10.0	9.7	62.5	23.1	9.7
11	8.7	12.6	7.2	11.2	15.5	11.6	10.4	17.2	12.0

The distributions 3 and 6 are not radially symmetric in contrast to the remaining distributions 1, 4, 6, and 11. For $\alpha = 1, 2$, the overall power of rejecting radial symmetry based on T_α^Y is above 75% for the investigated sample sizes. Merely $\alpha = 3$ needs more observations for a satisfyingly high power – arguably due to the lack of occurrences in the tightening sensitivity regions for small sample sizes (see section 3.2). For radially symmetric distributions, the choice of $\alpha = 2, 3$ leads to liberal test decisions for large sample sizes. However, for moderate sample sizes the choice of $\alpha = 2, 3$ can hold the desired level of 5% relatively well. All in all, $\alpha = 2$ seems to be a reasonable compromise in this kind of simulation study, resulting in high power and reasonable compliance of the level of error.

Although the tested distributions were quite artificially, a test based on T_α^Y is capable of

identifying the distributions with property **R**. The next section tests for radial symmetry if a sample is drawn from a bivariate copula.

4.2. Detecting radial symmetry in copulas

This section compares established nonparametric tests for radial symmetry, such as the one of Genest and Nešlehová (2014) which extends the work of Bouzebda and Cherfi (2012); Rosco and Joe (2013), of Li and Genton (2013), and of Krupskii (2016). Therefore, we benchmark the test based on the statistic T_α^Y against the test statistics S_n (Genest and Nešlehová, 2014) and G_R (Krupskii, 2016) in various scenarios.

First, it is investigated whether the level of error can be hold if a distribution is radially symmetric. For this purpose we use the radially symmetric Cauchy, Frank, and Gauss copula with parameters resulting in Kendall's $\tau = 0.25, 0.5, 0.75$ together with sample sizes $n = 100, 250, 500$. The simulated levels of S_n, G_R, and the new test for $\alpha = 1, 2, 3, 4$ are obtained from a Monte Carlo simulation with 1,000 iterations and listed in table 4. On the one hand, S_n and the new test are generally too conservative, especially for strong dependence and small sample sizes. On the other hand, a lower value of the parameter α tends to reject the Null of radial symmetry too often, especially if a sample is from a Cauchy copula. For moderate values of α and sufficiently large samples, both tests hold the level well. G_R performs consistently well for the Frank copula, independent of sample size, and especially for strong dependence, in which case the new test and S_n are relatively conservative. However, Krupskii (2016) does not show results for the other two investigated copula families.

Second, the three testing procedures for **R** are compared by their power in case of a sample drawn from a non radially symmetric copula family. Therefore, 1,000 samples of size $n = 100, 250, 500$ are drawn from the Clayton, the Gumbel, and the skew Student t copula with $\nu = 4$ and $a_1 = a_2 = 1$. The parameter of each distribution varies such that it results in a Kendall's $\tau = 0.25, 0.5, 0.75$. Again, S_n, G_R, and the new test for $\alpha = 1, 2, 3, 4$ are evaluated for each of the 1,000 samples, and the average rejection rate is calculated and reported in table 5.

Table 4: Simulated levels of S_n, G_R, and the new test for $\alpha_i = i$, $i = 1, 2, 3, 4$ for three copula families that are radially symmetric – the Cauchy (CA), the Frank (FR), and the Gauss copula (GA). Values (in %) are based on 1,000 Monte Carlo iterations, and reported for parameters that result in a dependence of $\tau = 0.25, 0.5, 0.75$ for sample sizes $n = 100, 250, 500$. The values of S_n and G_R are adopted from Genest and Nešlehová (2014) respectively Krupskii (2016) and therefore incomplete.

	$n = 100$						$n = 250$						$n = 500$					
	α_1	α_2	α_3	α_4	S_n	G_R	α_1	α_2	α_3	α_4	S_n	G_R	α_1	α_2	α_3	α_4	S_n	G_R
$\tau = 0.25$																		
CA	10.0	9.2	7.9	24.6	5.0	–	14.6	12.2	12.2	66.4	5.1	–	22.1	15.3	17.0	96.2	4.5	–
FR	4.1	4.1	3.8	3.6	3.8	4	8.3	6.6	5.8	6.3	3.5	6	13.2	7.6	7.1	3.9	3.4	4
GA	4.0	4.3	7.4	5.4	3.4	–	6.5	7.2	7.3	7.0	4.1	–	8.2	8.1	8.0	8.7	4.2	–
$\tau = 0.5$																		
CA	2.6	1.7	1.6	7.3	4.1	–	3.6	2.4	3.1	23.8	4.0	–	4.0	2.4	2.8	62.1	3.3	–
FR	2.5	3.3	5.8	8.8	4.0	5	6.6	3.2	6.8	10.2	3.6	6	12.7	5.5	6.1	9.5	3.4	5
GA	0.3	3.3	5.8	8.8	3.1	–	2.4	3.4	6.0	8.9	4.3	–	3.3	4.9	4.4	11.7	3.9	–
$\tau = 0.75$																		
CA	0.0	0.0	0.3	0.2	1.0	–	0.0	0.0	0.0	1.5	2.2	–	0.1	0.0	0.0	8.7	3.3	–
FR	0.0	0.0	0.9	3.8	0.9	4	0.0	0.2	1.3	6.8	2.1	4	0.0	0.1	1.0	9.9	2.9	6
GA	0.0	0.0	0.0	0.4	0.7	–	0.0	0.0	0.0	0.1	2.1	–	0.0	0.0	0.0	0.1	3.5	–

Table 5: Simulated power of S_n, G_R, and the new test for $\alpha_i = i$, $i = 1, 2, 3, 4$ for three copula families that are not radially symmetric – the Clayton (CL), the Gumbel (GU), and the skew Student t copula with $\nu = 4$ and $a_1 = a_2 = 1$ (S-t(4)). Values (in %) are based on 1,000 Monte Carlo iterations, and reported for parameters that result in a dependence of $\tau = 0.25, 0.5, 0.75$ for sample sizes $n = 100, 250, 500$. The values of S_n and G_R are adopted from Genest and Nešlehová (2014) respectively Krupskii (2016) and therefore incomplete.

	$n = 100$						$n = 250$						$n = 500$					
	α_1	α_2	α_3	α_4	S_n	G_R	α_1	α_2	α_3	α_4	S_n	G_R	α_1	α_2	α_3	α_4	S_n	G_R
$\tau = 0.25$																		
CL	17.9	53.5	53.8	47.5	35.1	50	52.9	93.7	90.8	88.1	72.3	87	84.4	100.0	99.6	99.6	94.9	99
S-t(4)	37.6	43.0	38.5	26.7	79.9	–	73.1	81.4	73.7	64.5	100.0	–	95.3	98.1	96.5	91.7	100.0	–
GU	17.5	13.6	19.5	25.7	7.9	21	46.4	38.0	45.7	52.0	19.2	47	81.0	59.1	71.0	79.9	46.5	79
$\tau = 0.5$																		
CL	23.3	85.2	91.5	89.7	71.3	92	79.8	100.0	100.0	100.0	99.5	100	99.2	100.0	100.0	100.0	100.0	100
S-t(4)	39.5	31.9	43.1	41.0	40.7	–	81.7	72.7	78.9	80.7	92.9	–	98.6	95.7	97.6	98.3	99.9	–
GU	13.9	13.8	28.4	35.9	12.2	36	52.6	40.9	68.3	79.3	42.9	74	89.7	77.3	95.2	97.5	76.3	98
$\tau = 0.75$																		
CL	0.2	41.9	69.9	86.2	72.8	98	2.2	97.9	99.8	100.0	100.0	100	34.5	100.0	100.0	100.0	100.0	100
S-t(4)	2.3	2.7	11.9	19.0	7.4	–	13.4	13.9	36.3	54.5	49.0	–	50.8	42.2	77.4	90.0	89.1	–
GU	0.0	0.0	1.8	7.5	5.8	27	0.2	0.8	11.4	36.7	36.4	79	2.6	6.1	49.6	88.0	78.7	99

If a sample is from the Clayton copula, this deviation can be detected best using G_R, for all n and τ. However, for larger n the new test with $\alpha > 1$ and S_n are performing equivalently. For the skew Student t copula, S_n outclasses the new test if the sample size is relatively small. If τ is fairly large however, the choice of $\alpha > 1$ results in a comparable power to S_n in detecting the radial symmetry. No results for G_R are available if the sample is drawn from the skew Student t distribution. It generally seems that deviations from radial symmetry induced by a sample from the Gumbel copula are detected more difficultly. However, for weak dependence, the new test is superior to S_n and G_R if the sample size is moderately large and $\alpha = 4 - G_R$ performs second and S_n has a low power in this setting. As τ increases moderately, the power of G_R and the new test increases simultaneously whereas the power of S_n decreases. For larger values of τ however, the power of S_n and the new test diminishes.

To summarize, the new test based on the statistic T_α^Y is suitable for detecting radial asymmetry of various kinds. It is comparable to established nonparametric testing procedures in the sense of a similar power. Apart from the intuitive geometrical understanding of the concept, the main advantage of using this new test is the fast examination time, since the distribution of the test statistic is easily determined and does not require critical values needs to be obtained by a preceded Monte Carlo simulation. In some situations, either the calculation time is limited or the mere number of tests that need to be carried out is large, which is especially true in the context of high dimensional vine copulas. In this case, a gain of calculation time per test can result in massive time savings. This aspect is further discussed in section 5.2.

4.3. Detecting asymmetry of the Azzalini copula

One class of skew t-copulas, first mentioned by Joe (2006), is based on the skew t-distribution by Azzalini and Capitanio (2003). In the centered bivariate case, four parameters need to be specified: a scale parameter θ, the degrees of freedom ν, and two skewness parameters a_1 and a_2. Aim of this section is testing for differences in deviations from independence in regions of the vertices due to asymmetry rather than radial symmetry. Thus, results are provided for T_α^X only. To isolate the effect of the parameters a_1 and a_2, the scale
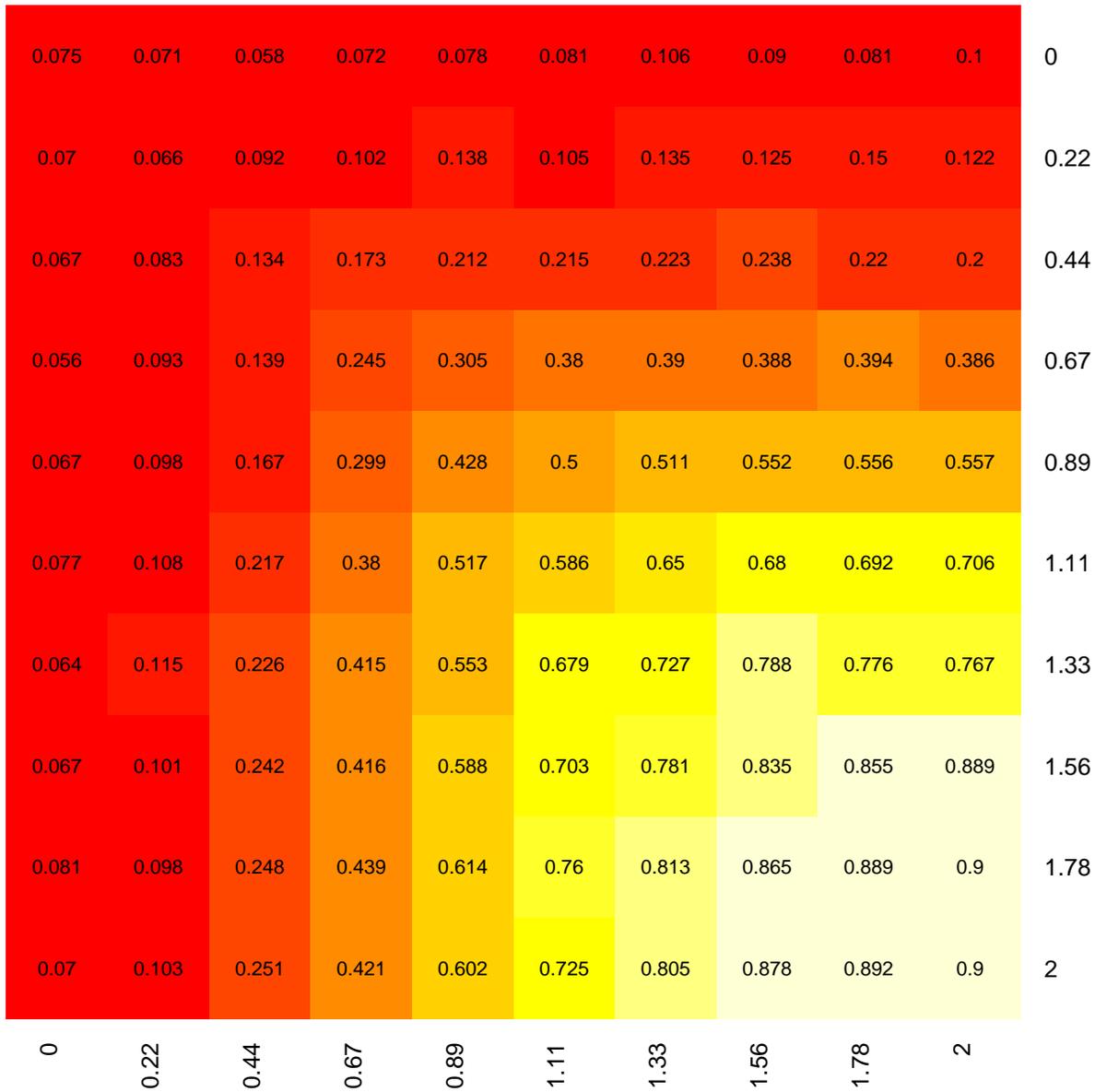
parameter θ is set to 0 in the following.

Figure 4: Simulated power of the test for vertex symmetry (level of error 5%, $c = 0.36$) for a sample of size $n = 100$ drawn from an Azzalini-type skew Student t copula with $\nu = 10$ and $\theta = 0$. Horizontal axis displays values of a_1, the vertical axis of a_2.

In a simulation study, level and power of the test based on T_α^X is analyzed if the sample is drawn from a bivariate Azzalini-type skew Student t copula with $\nu = 10$ and $\theta = 0$. The simulation results are based on 1,000 repetitions, samples of size $n = 100$ and skewness

23

parameters a_1, a_2, each varying from 0 to 2. The parameter α of the test of corollary 1 is set to $\alpha = 1$ which corresponds to $c = 0.36$ (see table 2). Figure 4 displays the power obtained by the test based on T_α^X.

The asymmetry can be detected well if both values of a_1, a_2 differ from zero (bright cells in figure 4). The more similar a_1 and a_2, the higher the power of the test. Notably, the power is very low if either one parameter, a_1, a_2, or both are close to zero – a parameter constellation that results in no skewness or univariate skewness only. Since the calculation of T_α^X is based on the ranks of a bivariate sample, skewness imputation that only affects one or no marginal distribution is canceled out. Therefore, only a parameter constellation that affects both marginal distributions simultaneously is detected well by this rank based testing procedure. Results for different values of ν, α, and θ require a more complex parameter iteration (as in Mangold (2015)) and are not provided in this paper.

In the following section, the new tests are applied to a real data set from the insurance market.

5. Application

The new tests from section 3.2 are now applied to an actuarial data set from Rosco and Joe (2013) to compare the conclusions regarding the symmetry in the data. Then, commonly used copula classes are categorized based on having the concepts **X** and/or **Y**. This distinction finds its application in the vine copula selection process of high dimensional vine structures.

5.1. Insurance

Here, T_α^X and T_α^Y are applied to a data set following Rosco and Joe (2013), who initially proposed a measure of tail asymmetry which later resulted in a test statistic for radial asymmetry of Genest and Nešlehová (2014). The data set contains 1,466 uncensored liability claims of an insurance company (see Frees and Valdez (1998) for a detailed description of the data): the loss resulting from an indemnity payment as well as the corresponding *Allocated Loss Adjustment Expense* (ALAE).
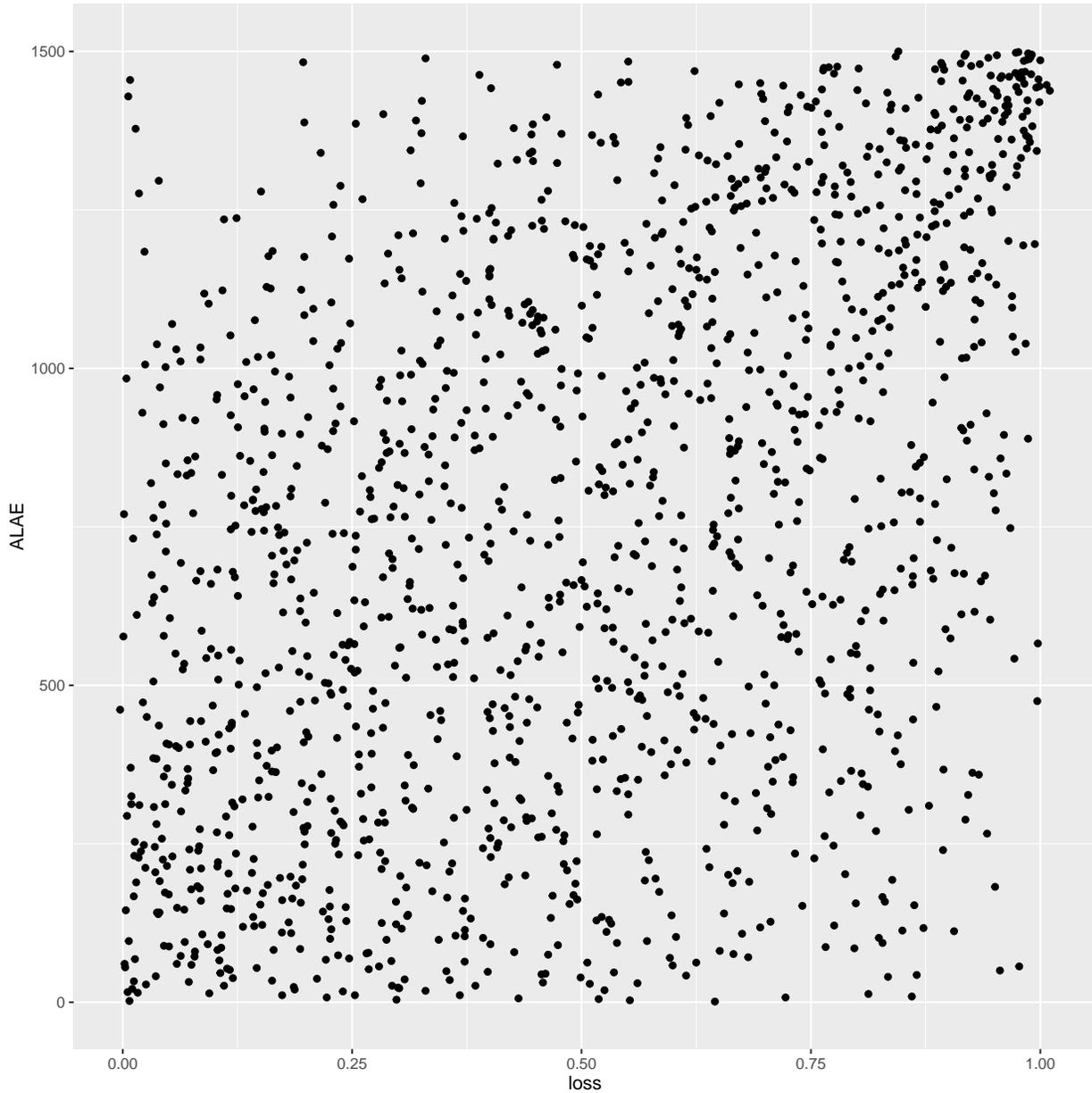
Figure 5: Indemnity payment (loss) and *Allocated Loss Adjustment Expense* (ALAE) of 1,466 liability claims (Frees and Valdez, 1998).

At first view on the scatterplot in figure 5, it seems that observations located close to vertex $(1,1)'$ have a higher density than close to vertex $(0,0)'$, implying a higher occurrence of joint upper tail observations (high loss combined with a high ALAE) than a lower tail observation (low loss combined with a low ALAE). This finding is underpinned by Rosco and Joe (2013), who find significantly positive tail asymmetry for the three new measures of tail

asymmetry. Surprisingly, there seems to be no difference between the density of occurrences near $(1,0)'$ (high loss, low ALAE) and $(0,1)'$ (low loss, high ALAE). It is suggested that the latter is less frequent than the the combination high loss, low ALAE. However, this problem is not tackled by Rosco and Joe (2013) but will be analyzed in the following.

First, the data is tested for vertex symmetry ($\mathbf{X}$), diametrical symmetry ($\mathbf{Y}$), and radial symmetry ($\mathbf{R}$). For values of $\alpha = 1, 2, 3, 4$, both $\mathbf{X}$ and $\mathbf{Y}$ are rejected at a level of error of 5%. Thus, referring to section 2.2, one can simultaneously reject $\mathbf{R}$, again at a level of 5%. Note that since differences in the components of $\boldsymbol{t}_\alpha$ are detected, H_0 of proposition 1 does not hold any longer. Therefore, the standard errors of the components of $\boldsymbol{t}_\alpha$ that are used for further analysis are obtained from 10,000 bootstrap samples.

Table 6 provides the results of two kinds of confidence intervals (CI, confidence level of 95% based on 10,000 bootstrap samples) of the standardized components of $\boldsymbol{t}_\alpha$, each associated to one vertex of $[0,1]^2$: CI_i containing bootstrapped values of one single component associated to $\boldsymbol{v}_i$, $i = 1, 2, 3, 4$, and $\text{CI}_{i,j}$ containing differences of two components associated to $\boldsymbol{v}_i$ and $\boldsymbol{v}_j$, $i, j = 1, 2, 3, 4$. E.g. 0 not being element of CI_1 indicates a substantial deviation from independence in $\boldsymbol{v}_1$. Further, e.g. $\text{CI}_{1,4}$ not containing 0 indicates that the deviations from independence in the vertices $\boldsymbol{v}_1$ and $\boldsymbol{v}_4$ are substantially different.

There seems to be a consistently substantial difference of $t_{\alpha,1}$ and $t_{\alpha,4}$ to zero, related to the upper and the lower bivariate tail, irrespective of the choice of α. Thus, in both tails an observation is more likely to occur than if the data's marginal distributions were independent. CI_2 and CI_3, corresponding to the remaining vertices $(0,1)'$ and $(1,0)'$, contain the value 0 only for values of $\alpha = 1, 2$. This indicates that the more regions located at the vertices are focused (by increasing α), the less the associated components of $\boldsymbol{t}_\alpha^s$ are distinguishable from zero. Note that due to the signs of the density values of the vertices in equation (5), the positive values of $t_{\alpha,2}$ and $t_{\alpha,3}$, related to the vertices $\boldsymbol{v}_2$ and $\boldsymbol{v}_3$, indicate a less likely occurrence than in the case of independence.

Next, the data is pairwisely analyzed regarding differences in $\boldsymbol{t}_\alpha^s$ between the upper/lower tail respectively between the vertices $(0,1)'$ and $(1,0)'$. Again, the results are presented in table 6. Irrespective of the choice of α, there is strong evidence for a difference in the tails corresponding to $(1,1)'$ and $(0,0)'$: Observations in the upper tail seems to occur more often

Table 6: Standardized values of $\boldsymbol{t}_\alpha$, where $\boldsymbol{v}_1 = (0,0)'$ corresponds to $t^s_{\alpha,4}$, $\boldsymbol{v}_4 = (1,1)'$ to $t^s_{\alpha,1}$, respectively $\boldsymbol{v}_2 = (0,1)'$ to $t^s_{\alpha,2}$, and $\boldsymbol{v}_3 = (1,0)'$ to $t^s_{\alpha,3}$. Simulated confidence intervals (CI, obtained using 10,000 bootstrap samples) based on the components of $\boldsymbol{t}^s_\alpha$ at a confidence level of 95%: Analysis if CI_i of a single component or $\mathrm{CI}_{i,j}$ of differences in two components contains the value 0, $i,j = 1,2,3,4$. E.g. $0 \notin \mathrm{CI}_1$ gives evidence for substantial deviation from independence in vertex $\boldsymbol{v}_1$, $0 \notin \mathrm{CI}_{1,2}$ indicates no difference in deviation from independence between $\boldsymbol{v}_1$ and $\boldsymbol{v}_4$.

Loss-ALAE	$\alpha = 1$				$\alpha = 2$			
	$\boldsymbol{v}_1$	$\boldsymbol{v}_4$	$\boldsymbol{v}_2$	$\boldsymbol{v}_3$	$\boldsymbol{v}_1$	$\boldsymbol{v}_4$	$\boldsymbol{v}_2$	$\boldsymbol{v}_3$
$\boldsymbol{t}^s_\alpha$	9.85	14.38	4.66	6.52	6.66	17.29	3.46	4.29
Standard error	0.91	0.77	0.52	0.50	0.65	1.44	0.42	0.38
$0 \notin \mathrm{CI}_i$	Yes	Yes	Yes	Yes	Yes	Yes	Yes	Yes
$0 \notin \mathrm{CI}_{i,j}$	Yes		No		Yes		No	
	$\alpha = 3$				$\alpha = 4$			
	$\boldsymbol{v}_1$	$\boldsymbol{v}_4$	$\boldsymbol{v}_2$	$\boldsymbol{v}_3$	$\boldsymbol{v}_1$	$\boldsymbol{v}_4$	$\boldsymbol{v}_2$	$\boldsymbol{v}_3$
$\boldsymbol{t}^s_\alpha$	4.87	15.87	1.59	1.39	3.74	14.65	0.47	-0.28
Standard error	0.82	1.38	0.20	0.59	1.30	1.04	0.49	0.26
$0 \notin \mathrm{CI}_i$	Yes	Yes	No	No	Yes	Yes	No	No
$0 \notin \mathrm{CI}_{i,j}$	Yes		No		Yes		No	

than in the lower tail. This result is essentially identical to the result of Rosco and Joe (2013), who find a significantly positive tail asymmetry based on evaluating their measure of skewness. Furthermore, $\mathrm{CI}_{2,3}$ does always contain the value 0, which indicates that there seems to be an identical deviation from independence within the regions close to $(0,1)'$ and $(1,0)'$ for any α.

Considering this finding, one would not choose a radially symmetric copula function for modeling the relationship between loss and ALAE, such as the Gaussian or Student t distribution. The next section gives an overview on families of bivariate copulas that are used in practice, mainly in the context of vine copulas, and classifies them according to the occurrence of the symmetry concepts $\mathbf{X}$ and $\mathbf{Y}$ from the definitions 5 and 6.

5.2. Vine copula selection

Nikoloulopoulos et al. (2012) classify copulas into six groups using different patterns of occurrence of tail dependencies. They propose that for diagnostic purposes, a range of copula families can be fitted to data and determine properties of the class containing the copula resulting in the smallest information criterion (e.g. AIC by Akaike (1974) or BIC by Schwarz (1978)). Then, the group that includes this copula is suggested to be adequate for the data. The six groups are: copulas with (a) tail independence, (b) intermediate tail dependence, (c) upper tail dependence only, (d) lower tail dependence only, (e) radial symmetry, (f) strong but different upper and lower tail dependence.

Turning the order around, one could use this classification scheme to downsize the computational expenditure in the vine copula selection process. Fitting a p-dimensional vine copula includes fitting $p(p-1)/2$ bivariate copulas out of a set of potential copula families. This is computationally cumbersome, especially for high dimensions and large sets of families. Addressing this problem, one could first test if there is some kind of symmetry in the data and then restrict the set of potential copula families to that group which possesses the tail dependence constellation that has been found in the data. Note that in the following rotations of copula models are allowed, which makes e.g. the Gumbel copula feasible for (c) with 0 degree rotation – and for (d) with 180 degrees rotation.

In each bivariate fitting step, the following set of decision rules could be applied in order to reduce computation time: At the beginning, start with a test for $\mathbf{X}$ and $\mathbf{Y}$. One of three possible constellations can occur: Firstly, if neither $\mathbf{X}$ nor $\mathbf{Y}$ can be rejected, a radially symmetric copula from (a), (b), or (e) should be fitted to the data, that gives the same probability to realizations within regions close to the vertices. Examples for such copula families are the independent, the Gauss, or the symmetric Student t copula, all with a dependence parameter close to zero or the parabola copula from remark 2. Secondly, if only $\mathbf{X}$ is rejected, it is suggested that realizations within regions close to diametrically opposed vertices occur with equal probability. Thus, copulas from (a), (b), or (e) (except the parabola copula), allowing for stronger dependencies, are suitable for the fitting process, along with rotations of 90, 180, and 270 degrees. Thirdly, if $\mathbf{X}$ and $\mathbf{Y}$ need to be rejected, there are several possible cases that can be identified comparing the entries of $\boldsymbol{t}_\alpha^s$ from section 5.1.

28

These are listed in table 7.

Table 7: Possible constellations if $\mathbf{X}$ and $\mathbf{Y}$ are rejected. $\boldsymbol{v}_i$, $i = 1, 2, 3, 4$, denotes the four vertices of the unit square $[0, 1]^2$: $\boldsymbol{v}_1 = (0, 0)'$, $\boldsymbol{v}_2 = (0, 1)'$, $\boldsymbol{v}_3 = (1, 0)'$, and $\boldsymbol{v}_4 = (1, 1)'$. The (in-)equality signs $>$, $<$ and $=$ are based on the CIs (confidence level 95%) that are constructed using the asymptotic distribution of $\boldsymbol{T}^\alpha$, e.g. $t^s_{\alpha,1} < t^s_{\alpha,4}$ holds if all values in $\mathrm{CI}_{1,4}$ are negative.

Cases	$\boldsymbol{t}^s_\alpha$				Rotations (degrees)			
	$\boldsymbol{v}_1$	$\boldsymbol{v}_4$	$\boldsymbol{v}_3$	$\boldsymbol{v}_2$	0	90	180	270
I	$t^s_{\alpha,1} <$	$t^s_{\alpha,4}$ and	$t^s_{\alpha,3} =$	$t^s_{\alpha,2}$	(c)(f)	-	(d)(f)	-
II	$t^s_{\alpha,1} >$	$t^s_{\alpha,4}$ and	$t^s_{\alpha,3} =$	$t^s_{\alpha,2}$	(d)(f)	-	(c)(f)	-
III	$t^s_{\alpha,1} =$	$t^s_{\alpha,4}$ and	$t^s_{\alpha,3} >$	$t^s_{\alpha,2}$	-	(c)(f)	-	(d)(f)
IV	$t^s_{\alpha,1} =$	$t^s_{\alpha,4}$ and	$t^s_{\alpha,3} <$	$t^s_{\alpha,2}$	-	(d)(f)	-	(c)(f)
V	any other constellation				best fit (a) – (e), all rotations			

Note that as an example in case I, having a heavier upper tail with rotation 0 degrees is equivalent to having a heavier lower tail with 180 degrees rotation. Fourthly, if case V of table 7 is selected, all potentially feasible copulas are fitted to the data with every rotation and the family that results in the smallest information criterion is selected.

6. Outlook

In this article two new concepts of symmetry for bivariate copulas, $\mathbf{X}$ and $\mathbf{Y}$, have been introduced. Both concepts are focused on regions of the unit square $[0, 1]^2$ that are located near the four vertices. A copula has the property $\mathbf{X}$, if the probability of an observation in a square located in each vertex is equally likely. The property $\mathbf{Y}$ characterizes a copula in which probabilities of an observation in a square located in diametrically opposed vertices is equally likely. It has been shown, that the new concept $\mathbf{Y}$ is related to radial symmetry ($\mathbf{R}$), which is supposed to be the most natural form of symmetry for copulas (Nelsen, 1993). If a copula does not exhibits $\mathbf{Y}$, it can be concluded that $\mathbf{R}$ is neither possessed.

A new generalization of the FGM-copula has been introduced that allows to model the probabilistic behavior in each tail of arbitrary dimension separately using one parameter

each. Due to the curse of dimensionality and admissibility restrictions of the parameters, classical estimation procedures fail if information about every parameter is deducted from data. Thus, a vector $\boldsymbol{T}_\alpha$ containing a collection of locally most powerful rank tests for independence has been derived for each single parameter, associated to one and only one vertex (following Garralda-Guillén (1998), Genest and Verret (2005), and Mangold (2015)). Even though the entries of $\boldsymbol{T}_\alpha$ itself cannot be interpreted as parameters of the polynomial copula anymore, they provide information on whether or not occurrences within a region close to the vertices are more or less likely than in the case of independence. Deviations from this probability under independence can be compared among one another and have been used used to test for the two new symmetry concepts $\mathbf{X}$, $\mathbf{Y}$, and radial symmetry. A connection between the additional parameter of the polynomial copula family and the symmetry concepts $\mathbf{X}$ and $\mathbf{Y}$ has been motivated.

In several simulation studies the power of the test for diametrical symmetry as a test for radial symmetry has been analyzed. First, several constellations of three other symmetries for copulas have been considered and the power of the new test for radial symmetry has been inspected. Second, the power of the new test has been compared to that of other nonparametric tests of radial symmetry that are of interest in recent literature (see Genest and Nešlehová (2014), Krupskii (2016)). Third, the power of the test for vertex symmetry has been examined in case a sample is drawn from a bivariate skew Azzalini-type Student t copula (Azzalini and Capitanio, 2003; Joe, 2006) to detect skewness in the data. In all three simulations, the new tests show considerably large power in combination with short calculation time, which can justify the usage of the new procedures in practical applications.

The realization $\boldsymbol{t}_\alpha^s$ has been calculated for a data set from the insurance sector (Frees and Valdez, 1998), and conclusions based on T_α^X, T_α^Y, and by comparing differences in the entries of $\boldsymbol{t}_\alpha^s$ have been drawn. It has been shown that the conclusions are identical to those based on other state-of-the-art measures for asymmetry in tails (see Rosco and Joe (2013)).

Subsequently, a possible improvement of the selection process employed by vine copula fitting procedures has been proposed, eliminating copulas from a set of potential candidates that do not inherit the symmetry structure which was found in the data (following Nikoloulopoulos et al. (2012)). This approach focuses high dimensional vine copula fitting

processes, for which reduction of calculation time is crucial due to the exponentially increasing amount of pairwise copulas that need to be fitted.

Overall, testing for radial symmetry using T_α^Y seems to be a viable alternative to other state-of-the-art tests, due to the fast calculation of critical values or p-values of the χ^2-distribution, and hence the test decision. Regular nonparametric tests for radial symmetry require a computationally time intense Monte Carlo simulation for determining critical values which can be a knock-out criterion in time critical applications and/or high dimensions. Note that having introduced the new concepts of symmetry in the bivariate case only, a generalization to arbitrary dimensions is straightforward while remaining intuitive: For a p-dimensional copula, the property $\mathbf{X}$ is equivalent to having the identical probability of observing an outcome within areas located in every vertex of the unitcube $[0,1]^p$. $\mathbf{Y}$ stands for the identical probability of observing an outcome within areas located in vertices of $[0,1]^p$ that are diametrically opposed. A test for $\mathbf{X}$ for a p-dimensional copula compares $t_{\alpha,i} \approx t_{\alpha,j}$, $i \neq j$, $i,j = 1,...,p$, while a test for $\mathbf{Y}$ would compare $t_{\alpha,j} \approx t_{\alpha,d-j+1} \forall j \in 1,...,2^{p-1}$. Even in dimensions $p \gg 2$, testing for vertex and diametrical symmetry is possible with few computational effort. This poses a sound alternative to previous approaches on handling symmetry in higher dimensions, as pairwise radial symmetry, and will be subject of further research.

Software

All calculations and graphics have been accomplished using R (R Core Team, 2016, version 3.3.1) including the packages listed in table 8.

Bibliography

Akaike, H. (1974). A new look at the statistical model identification. *IEEE Transactions on Automatic Control*, 19(6):716–723.

Auguie, B. (2016). *gridExtra: Miscellaneous Functions for "Grid" Graphics*. R package version 2.2.1.

Table 8: `R`-packages used for calculations and graphics.

`R` package	Authors of the `R` package
copula	Hofert et al. (2016)
dplyr	Wickham and Francois (2016)
ggplot2	Wickham (2009)
gridExtra	Auguie (2016)
Hmisc	Harrell Jr et al. (2016)
Rcpp	Eddelbuettel and Francois (2016)
sn	Azzalini (2016)

Azzalini, A. (2016). *The R package sn: The Skew-Normal and Skew-t distributions*. Università di Padova, Padua. R package version 1.4-0.

Azzalini, A. and Capitanio, A. (2003). Distributions generated by perturbation of symmetry with emphasis on a multivariate skew t-distribution. *Journal of the Royal Statistical Society: Series B (Statistical Methodology)*, 65(2):367–389.

Barnett, V. (1980). Some bivariate uniform distributions. *Communications in Statistics - Theory and Methods*, 9(4):453–461.

Bedford, T. and Cooke, R. M. (2001). Probability density decomposition for conditionally dependent random variables modeled by vines. *Annals of Mathematics and Artificial Intelligence*, 32(1):245–268.

Bedford, T. and Cooke, R. M. (2002). Vines: A new graphical model for dependent random variables. *Annals of Statistics*, 30(4):1031–1068.

Bouzebda, S. and Cherfi, M. (2012). Test of symmetry based on copula function. *Journal of Statistical Planning and Inference*, 142(5):1262–1271.

Brechmann, E. C. and Czado, C. (2013). Risk management with high-dimensional vine copulas: An analysis of the Euro Stoxx 50. *Statistics & Risk Modeling*, 30(4):307–342.

Brechmann, E. C., Czado, C., and Aas, K. (2012). Truncated regular vines in high dimensions with application to financial data. *Canadian Journal of Statistics*, 40(1):68–85.

Clayton, D. G. (1978). A model for association in bivariate life tables and its application in epidemiological studies of familial tendency in chronic disease incidence. *Biometrika*, 65(1):141–151.

Czado, C. (2010). Pair-copula constructions of multivariate copulas. In Jaworski, P., Durante, F., Härdle, W. K., and Rychlik, T., editors, *Copula Theory and its Applications: Proceedings of the Workshop held in Warsaw, 25-26 September 2009*, pages 93–109. Springer, Berlin/Heidelberg, Germany.

Eddelbuettel, D. and Francois, R. (2016). *Rcpp: Seamless R and C++ integration.* R package version 0.12.7.

Fang, H.-B., Fang, K.-T., and Kotz, S. (2002). The meta-elliptical distributions with given marginals. *Journal of Multivariate Analysis*, 82(1):1–16.

Farlie, D. J. G. (1960). The performance of some correlation coefficients for a general bivariate distribution. *Biometrika*, 47(3/4):307–323.

Fréchet, M. (1958). Remarques au sujet de la note précédente. *Comptes Rendus de l'Académie des Sciences Paris*, 246:2719–2720.

Frees, E. W. and Valdez, E. A. (1998). Understanding relationships using copulas. *North American Actuarial Journal*, 2(1):1–25.

Garralda-Guillén, A. I. (1998). Dependencia y tests de rangos para leyes bidimensionales. *Doctoral thesis, Universidad de Granada, Spain.*

Genest, C., Favre, A.-C., Béliveau, J., and Jacques, C. (2007). Metaelliptical copulas and their use in frequency analysis of multivariate hydrological data. *Water Resources Research*, 43(9).

Genest, C. and Nešlehová, J. G. (2014). On tests of radial symmetry for bivariate copulas. *Statistical Papers*, 55(4):1107–1119.

Genest, C., Nešlehová, J. G., and Quessy, J.-F. (2012). Tests of symmetry for bivariate copulas. *Annals of the Institute of Statistical Mathematics*, 64(4):811–834.

Genest, C. and Verret, F. (2005). Locally most powerful rank tests of independence for copula models. *Journal of Nonparametric Statistics*, 17(5):521–539.

Guégan, D. and Hassani, B. K. (2013). Multivariate VaRs for operational risk capital computation: A vine structure approach. *International Journal of Risk Assessment and Management*, 17(2):148–170.

Guégan, D. and Maugis, P. A. (2010). New prospects on vines. *Insurance Markets and Companies: Analyses and Actuarial Computations*, 1(1):4–11.

Gumbel, E. J. (1960). Bivariate exponential distributions. *Journal of the American Statistical Association*, 55(292):698–707.

Gyasi-Agyei, Y. (2011). Copula-based daily rainfall disaggregation model. *Water Resources Research*, 47(7).

Hampel, F. R. (1986). *Robust Statistics: The Approach based on Influence Functions*. Wiley series in probability and mathematical statistics. Wiley, New York, USA.

Harrell Jr, F. E., with contributions from Charles Dupont, and many others (2016). *Hmisc: Harrell Miscellaneous*. R package version 3.17-4.

Hofert, M., Kojadinovic, I., Mächler, M., and Yan, J. (2016). *copula: Multivariate dependence with copulas*. R package version 0.999-15.

Hua, L. and Joe, H. (2011). Tail order and intermediate tail dependence of multivariate copulas. *Journal of Multivariate Analysis*, 102(10):1454–1471.

Joe, H. (1993). Parametric families of multivariate distributions with given margins. *Journal of Multivariate Analysis*, 46(2):262–282.

Joe, H. (1996). Families of m-variate distributions with given margins and $m(m-1)/2$ bivariate dependence parameters. In Rüschendorf, L., Schweizer, B., and Taylor, M. D.,

editors, *Distributions with Fixed Marginals and Related Topics*, pages 120–141. Institute of Mathematical Statistics, Hayward, USA.

Joe, H. (1997). *Multivariate Models and Multivariate Dependence Concepts*, volume 73 of *Monographs on Statistics and Applied Probability*. CRC Press, Boca Raton, USA.

Joe, H. (2006). Discussion of "Copulas: Tales and facts", by Thomas Mikosch. *Extremes*, 9(1):37–41.

Klein, I. and Fischer, M. (2004). Tailabhängigkeit und Asymmetrie in multivariaten Finanzmarktdaten. In *Finanzintermediation: Theoretische, wirtschaftspolitische und praktische Aspekte aktueller Entwicklungen im Bank- und Börsenwesen*, pages 69–101. Schäffer-Poeschel, Stuttgart, Germany.

Krupskii, P. (2016). Copula-based measures of reflection and permutation asymmetry and statistical tests. *Statistical Papers*, pages 1–23.

Lau, C. A., Xie, W., and Wu, Y. (2016). Multi-dimensional pairs trading using copulas. *Working paper, Nanyang Technological University, Singapore*.

Li, B. and Genton, M. G. (2013). Nonparametric identification of copula structures. *Journal of the American Statistical Association*, 108(502):666–675.

Low, R. K. Y., Alcock, J., Faff, R., and Brailsford, T. (2013). Canonical vine copulas in the context of modern portfolio management: Are they worth it? *Journal of Banking & Finance*, 37(8):3085–3099.

Mangold, B. (2015). A multivariate linear rank test of independence based on a multiparametric polynomial copula. IWQW Discussion Paper Series 10, Friedrich-Alexander University Erlangen-Nürnberg, Germany.

Morgenstern, D. (1956). Einfache Beispiele zweidimensionaler Verteilungen. *Mitteilungsblatt für Mathematische Statistik*, 8(1):234–235.

Nelsen, R. B. (1993). Some concepts of bivariate symmetry. *Journal of Nonparametric Statistics*, 3(1):95–101.

Nelsen, R. B. (2006). *An Introduction to Copulas.* Springer series in statistics. Springer, New York, USA, 2nd edition.

Nelsen, R. B., Quesada-Molina, J. J., and Rodriguez-Lallena, J. A. (1997). Bivariate copulas with cubic sections. *Journal of Nonparametric Statistics*, 7(3):205–220.

Nikoloulopoulos, A. K., Joe, H., and Li, H. (2012). Vine copulas with asymmetric tail dependence and applications to financial return data. *Computational Statistics & Data Analysis*, 56(11):3659–3673.

R Core Team (2016). *R: A Language and Environment for Statistical Computing.* R Foundation for Statistical Computing, Vienna.

Rosco, J. F. and Joe, H. (2013). Measures of tail asymmetry for bivariate copulas. *Statistical Papers*, 54(3):709–726.

Schwarz, G. (1978). Estimating the dimension of a model. *The Annals of Statistics*, 6(2):461–464.

Sklar, M. (1959). Fonctions de répartition à n dimensions et leurs marges. *Publications de l'Institut de Statistique de l'Université de Paris*, 8:229–231.

Stübinger, J., Mangold, B., and Krauß, C. (2016). Statistical arbitrage with vine copulas. FAU Discussion Papers in Economics 11, Friedrich-Alexander University Erlangen-Nürnberg, Germany.

Weiß, G. N. F. and Supper, H. (2013). Forecasting liquidity-adjusted intraday Value-at-Risk with vine copulas. *Journal of Banking & Finance*, 37(9):3334–3350.

Wickham, H. (2009). *ggplot2: Elegant Graphics for Data Analysis.* Springer, New York, USA.

Wickham, H. and Francois, R. (2016). *dplyr: A grammar of data manipulation.* R package version 0.5.0.
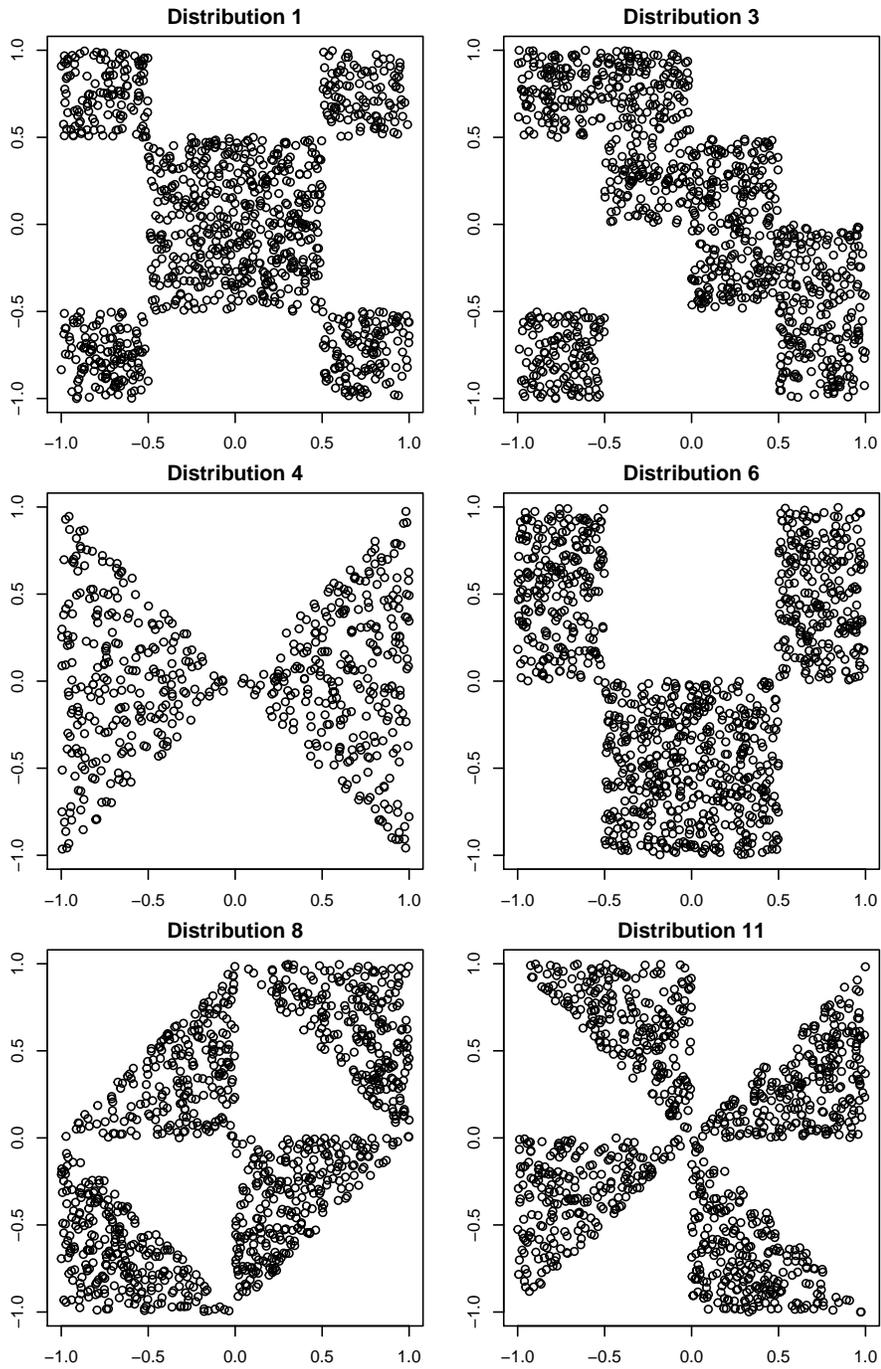
Appendix

Figure 6: Scatterplot of a random sample of distributions that have the constellations of symmetry listed in table 1.